

## Response to review

Dear Editor

I have gone through the reviewer's comments and fully agree that the description of the SE calculations has not been good enough. The confusion stems from a combination of a few mistakes in the 'n' number and the description of how it was calculated.

I have carefully gone through the manuscript and made appropriate corrections/changes, mainly in the materials and methods chapter and the Table and Figure legends. When going through the manuscript again I found a few minor things (e.g. spelling) that were also corrected in this version. A detailed response to each point is given below, plus the full manuscript with track changes.

Sincerely,

Kristian Spilling

## All the issues and points raised by the reviewer followed with our response

I am afraid I still don't understand correctly as it seems that answers provided and the new paragraph that was added do not match. If I understand correctly, rates of change (i.e. Delta DOC) were calculated as the difference between the start (2 first days) of each period. **My first question would be: how did you do for the last period?**

**Author response** – it was done from the average of the last two days and this information has been added to the text (M&M chapter) and to the Table 3 legend.

In the added paragraph, it does not seem to be explained correctly. The same is true for the legends of Table 1-3, as it is said that: "... net community production estimated based on organic carbon pools (NCPo) are all average for Phase I in mmol C m<sup>-2</sup> d<sup>-1</sup> ± SE (n = 16)." **How can you have n = 16 if based on a difference between 2 time points?**

**Author response** – It was not based on the difference between two time points, as all variables were measured throughout the different phases, and the SE was calculated from the full set of data (please see also our explanation to your example of DOC below). You are right that the n = 16 is inaccurate. NCPo was calculated based on Eq. 5, for all the measured variables we have now placed the exact n number (it was 16 only for TR).

**Moreover, regarding measured rates (i.e. BP), I doubt that they were measured on a daily basis (n is not 16), but I might be wrong.**

**Author response** – You are partly right. NPP and TR were measured on a daily basis (but with a loss of some number of NPP as the incubation platform at some point disappeared),

but other parameters including BP was measured every 2-3 days. In the figure legend we now specify the exact n for all variables.

If I take the example of Delta DOC in M1 for Phase 1, that would be 16.4 mmol C/m<sup>2</sup>/d (considering a 16 day period, 7435 for the start of phase 1 - 7172 for the start of phase 2), a value of 15.5 is reported. I end up with a NCPo estimate of 18.2 mmol C/m<sup>2</sup>/d.

**Author response** – Phase I, M1: the total period counted was from t0 to t16, which is 17 days when including day 0 as the first day, ending up with 15.5 instead of 16.4. This affects also NCPo.

More importantly, I don't understand that, if indeed you propagated errors the way you explained (i.e. square root of the sum of variance), how you end up with a propagated error that is lower than one of the terms. For instance, still for M1 in Phase 1, delta DOC should have an error of  $\text{SQRT}(87^2+38^2) = \text{ca. } 95$ . Doing the same for delta TPC (SE ~40), you would end up with a propagated error on NCPo of  $\text{SQRT}(95^2+40^2+0.1^2) = 103$ , far from the value of 33 that is reported.

**Author response** –The confusion most likely stems from an error in the n value set for the Delta ( $\Delta$ ) variables, and that the explanation of SE calculations was not elaborate enough. In your given example the n value is 8 and not 2. The SE for the  $\Delta$  variables was not calculated from SE of the pools, e.g.  $\text{DOC}_{\text{pool}}$  as in your example. Rather, the change was calculated between each measuring point and the SE for  $\Delta$  variables calculated for the full range. We have corrected the n value in the figure legend, and elaborated the description in the materials and methods chapter.

I might have misunderstood, however if this is the case, first I apologize, but also I would suggest the authors to better clarify their methodology.

**Author response** - We fully agree and have hopefully managed to make the description of the SE calculations clear.

Very minor corrections:

L18-21: Affiliations have been swapped

**Author response** – Corrected

L50: Please remove “fixed”

**Author response** – removed

L180: A parenthesis is missing in the equation

**Author response** – corrected

L650: since you calculate GPP from your budgets, you should change to: (i.e. NCP + TR)

**Author response** - L650 is in the reference section, I looked through all places where GPP appeared, but did not find any apparent place where '(i.e. NCP + TR)' should be inserted.

1 Effects of ocean acidification on pelagic carbon fluxes in a  
2 mesocosm experiment

3  
4

5 Kristian Spilling<sup>1,2</sup>, Kai G. Schulz<sup>3</sup>, Allannah J. Paul<sup>4</sup>, Tim Boxhammer<sup>4</sup>, Eric P. Achterberg<sup>4,</sup>  
6 <sup>5</sup>, Thomas Hornick<sup>6</sup>, Silke Lischka<sup>4</sup>, Annegret Stuhr<sup>4</sup>, Rafael Bermúdez<sup>4,7</sup>, Jan Czerny<sup>4</sup>, Kate  
7 Crawford<sup>8</sup>, Corina P. D. Brussaard<sup>8,9</sup>, Hans-Peter Grossart<sup>6,10</sup>, Ulf Riebesell<sup>4</sup>

8 [1] {Marine Research Centre, Finnish Environment Institute, P.O. Box 140, 00251 Helsinki,  
9 Finland}

10 [2] {Tvärminne Zoological Station, University of Helsinki, J. A. Palménin tie 260, 10900  
11 Hanko, Finland}

12 [3] {Centre for Coastal Biogeochemistry, Southern Cross University, Military Road, East  
13 Lismore, NSW 2480, Australia}

14 [4] {GEOMAR Helmholtz Centre for Ocean Research Kiel, Düsternbrooker Weg 20, 24105  
15 Kiel, Germany}

16 [5] {National Oceanography Centre Southampton, European Way, University of  
17 Southampton, Southampton, SO14 3ZH, UK}

18 [[6](#)] {[Leibniz Institute of Freshwater Ecology and Inland Fisheries \(IGB\), Experimental](#)  
19 [Limnology, 16775 Stechlin, Germany](#)}

20 [7] {Facultad de Ingeniería Marítima, Ciencias Biológicas, Oceánicas y Recursos Naturales.  
21 ESPOL, Escuela Superior Politécnica del Litoral, Guayaquil, Ecuador}

22 [~~6~~] {~~Leibniz Institute of Freshwater Ecology and Inland Fisheries (IGB), Experimental~~  
23 ~~Limnology, 16775 Stechlin, Germany~~}

24 [8] {NIOZ Royal Netherlands Institute for Sea Research, Department of Marine  
25 Microbiology and Biogeochemistry, and Utrecht University, P.O. Box 59, 1790 AB Den  
26 Burg, Texel, The Netherlands}

27 [9] {Department of Aquatic Microbiology, Institute for Biodiversity and Ecosystem  
28 Dynamics (IBED), University of Amsterdam, The Netherlands}

29 [10] {Potsdam University, Institute for Biochemistry and Biology, 14469 Potsdam,  
30 Germany}

31

32 Correspondence to: K. Spilling (kristian.spilling@environment.fi)

33 Running title: Modified pelagic carbon fluxes

34 Key words: Carbon fluxes, carbon budget, gross primary production, respiration, bacterial  
35 production, sinking carbon flux, CO<sub>2</sub> exchange with atmosphere

36 **Abstract**

37 About a quarter of anthropogenic CO<sub>2</sub> emissions are currently taken up by the oceans  
38 decreasing seawater pH. We performed a mesocosm experiment in the Baltic Sea in order to  
39 investigate the consequences of increasing CO<sub>2</sub> levels on pelagic carbon fluxes. A gradient of  
40 different CO<sub>2</sub> scenarios, ranging from ambient (~370 μatm) to high (~1200 μatm), were set  
41 up in mesocosm bags (~55 m<sup>3</sup>). We determined standing stocks and temporal changes of total  
42 particulate carbon (TPC), dissolved organic carbon (DOC), dissolved inorganic carbon (DIC)  
43 and particulate organic carbon (POC) of specific plankton groups. We also measured carbon  
44 flux via CO<sub>2</sub> exchange with the atmosphere and sedimentation (export); and biological rate  
45 measurements of primary production, bacterial production and total respiration. The  
46 experiment lasted for 44 days and was divided into three different phases (I: *t0-t16*; II: *t17-*  
47 *t30*; III: *t31-t43*). Pools of TPC, DOC and DIC were approximately 420, 7200 and 25200  
48 mmol C m<sup>-2</sup> at the start of the experiment, and the initial CO<sub>2</sub> additions increased the DIC  
49 pool by ~7% in the highest CO<sub>2</sub> treatment. Overall, there was a decrease in TPC and increase  
50 of DOC over the course of the experiment. The decrease in TPC was lower, and increase in  
51 DOC higher, in treatments with added CO<sub>2</sub>. During Phase I the estimated gross primary  
52 production (GPP) was ~100 mmol C fixed-m<sup>-2</sup> d<sup>-1</sup>; from which 75-95% were respired, ~1%  
53 ended up in the TPC (including export) and 5-25% added to the DOC pool. During Phase II,  
54 the respiration loss increased to ~100% of GPP at the ambient CO<sub>2</sub> concentration, whereas  
55 respiration was lower (85-95% of GPP) in the highest CO<sub>2</sub> treatment. Bacterial production  
56 was ~30% lower, on average, at the highest CO<sub>2</sub> concentration compared with the controls  
57 during Phases II and III. This resulted in a higher accumulation DOC standing stock and  
58 lower reduction in TPC in the elevated CO<sub>2</sub> treatments at the end of Phase II extending  
59 throughout Phase III. The “extra” organic carbon at high CO<sub>2</sub> remained fixed in an increasing  
60 biomass of small-sized plankton and in the DOC pool, and did not transfer into large, sinking  
61 aggregates. Our results revealed a clear effect of increasing CO<sub>2</sub> on the carbon budget and  
62 mineralization, in particular under nutrient limited conditions. Lower carbon loss processes  
63 (respiration and bacterial remineralization) at elevated CO<sub>2</sub> levels resulted in higher TPC and  
64 DOC pools compared with the ambient CO<sub>2</sub> concentration. These results highlight the  
65 importance to address not only net changes in carbon standing stocks, but also carbon fluxes  
66 and budgets to better disentangle the effects of ocean acidification.

67

68 **1 Introduction**

69 Combustion of fossil fuels and change in land use, have caused increasing atmospheric  
70 concentrations of carbon dioxide (CO<sub>2</sub>). Ca. 25% of the anthropogenic CO<sub>2</sub> is absorbed by  
71 the oceans, thereby decreasing surface water pH, a process termed ocean acidification (Le  
72 Quéré et al., 2009). Ocean acidification and its alterations of aquatic ecosystems have  
73 received considerable attention during the past decade, but there are many open questions, in  
74 particular related to consequences for planktonic mediated carbon fluxes.

75 Some studies on ocean acidification have reported increased carbon fixation (Egge et al.,  
76 2009; Engel et al., 2013), bacterial production (Grossart et al., 2006) and bacterial  
77 degradation of polysaccharides (Piontek et al., 2010) at enhanced CO<sub>2</sub> levels, with potential  
78 consequences for carbon fluxes within pelagic ecosystems and export to the deep ocean, i.e.  
79 the biological carbon pump. Increasing carbon fixation in a high CO<sub>2</sub> environment can  
80 translate into an enhanced sequestration of carbon (Riebesell et al., 2007), but this depends on  
81 numerous environmental factors including phytoplankton community composition, aggregate  
82 formation and nutrient availability. For example, if the community shifts towards smaller cell  
83 sizes and/or enhanced cycling of organic matter carbon, export from the upper water layers  
84 may decrease (Czerny et al., 2013a).

85 The effect of ocean acidification has mostly been studied in marine ecosystems under high  
86 phytoplankton biomass. Brackish water has lower buffering capacity than ocean water and  
87 the pH fluctuates more. The limited number of studies of ocean acidification in brackish  
88 water and indications that ocean acidification effects are greatest under nutrient limitation  
89 (De Kluijver et al., 2010), motivated this mesocosm study in the Baltic Sea during low  
90 nutrient, summer months.

91 The Baltic Sea is functionally much like a large estuary, with a salinity gradient  
92 ranging from approximately 20 in the South-West to <3 in the Northernmost Bothnian Bay. It  
93 is an almost landlocked body of water with a large population in its vicinity (~80 million).  
94 Human activities (e.g. agriculture, shipping and fishing) cause a number of environmental  
95 problems such as eutrophication and pollution. As a coastal sea projected to change rapidly  
96 due to interaction of direct and indirect anthropogenic pressures, the Baltic Sea can be seen as  
97 a model ecosystem to study global change scenarios (Niiranen et al., 2013).

98 Most primary data from this experiment are published in several papers of this Special Issue  
99 (Riebesell et al., 2015). The aim of the present paper is to provide an overarching synthesis of

100 all information related to carbon standing stocks and fluxes. This enabled us to calculate  
101 carbon budgets in relation to different CO<sub>2</sub> levels.

102

103

## 104 **2 Materials and methods**

105

### 106 **2.1. Experimental set-up**

107 Six Kiel Off-Shore Mesocosms for future Ocean Simulations (KOSMOS; with a volume of  
108 ca. 55 m<sup>3</sup>) were moored at Storfjärden, on the south west coast of Finland (59° 51.5' N; 23°  
109 15.5' E) on 12 June 2012 (nine KOSMOS units were originally deployed but three were lost  
110 due to leaks). A more detailed description of the set-up can be found in Paul et al. (2015).

111 The mesocosms extended from the surface down to 19 m depth and had a conical bottom end,  
112 which enabled quantitative collection of the settling material. Different CO<sub>2</sub> levels in the bags  
113 were achieved by adding filtered (50 µm), CO<sub>2</sub>-saturated seawater. The CO<sub>2</sub> enriched water  
114 was evenly distributed over the upper 17 m of the water columns and added in 4 consecutive  
115 time steps (*t*<sub>0</sub> – *t*<sub>3</sub>). Two controls and four treatments were used, and for the controls, filtered  
116 seawater (without additional CO<sub>2</sub> enrichment) was added. The CO<sub>2</sub> fugacity gradient after all  
117 additions ranged from ambient (average throughout the experiment: ~370 µatm *f*CO<sub>2</sub>) in the  
118 two control mesocosms (M1 and M5), up to ~1200 µatm *f*CO<sub>2</sub> in the highest treatment (M8).  
119 We used the average *f*CO<sub>2</sub> throughout this experiment (from *t*<sub>1</sub> – *t*<sub>3</sub>) to denote the different  
120 treatments: 365 (M1), 368 (M5), 497 (M7), 821 (M6), 1007 (M3) and 1231 (M8) µatm *f*CO<sub>2</sub>.  
121 On *t*<sub>15</sub>, additional CO<sub>2</sub>-saturated seawater was added to the upper 7 m in the same manner as  
122 the initial enrichment, to counteract outgassing of CO<sub>2</sub>.

123 We sampled the mesocosm every morning, but some variables were determined only every  
124 second day. Depth-integrated water samples (0 – 17 m) were taken by using integrating water  
125 samplers (IWS, HYDRO-BIOS, Kiel). The water was collected into plastic carboys (10 L)  
126 and taken to the laboratory for sub-sampling and subsequent determination of carbon stocks.

127

### 128 **2.2. Primary variables**

129 For more detailed descriptions of the primary variables and the different methods used during  
130 this CO<sub>2</sub> mesocosm campaign, we refer to other papers in this joint volume: i.e. total  
131 particulate carbon (TPC), dissolved organic carbon (DOC), and dissolved inorganic carbon  
132 (DIC) are described by Paul et al. (2015); micro and nanophytoplankton enumeration by  
133 Bermúdez et al. (2016); picophytoplankton, heterotrophic prokaryotes and viruses by  
134 Crawford et al. (2016); zooplankton community by Lischka et al. (2015); primary production  
135 and respiration by Spilling et al. (2016); bacterial production (BP) by Hornick et al. (2016);  
136 and sedimentation by Boxhammer et al. (2016); and Paul et al. (2015).

137 Briefly, samples for TPC (500 mL) were GF/F filtered and determined using an elemental  
138 analyzer (EuroAE). DOC was measured using the high temperature combustion method  
139 (Shimadzu TOC –VCPN) following Badr et al. (2003). DIC was determined by infrared  
140 absorption (LI-COR LI-7000 on an AIRICA system). The DIC concentrations were  
141 converted from  $\mu\text{mol kg}^{-1}$  to  $\mu\text{mol L}^{-1}$  using the average seawater density of  $1.0038 \text{ kg L}^{-1}$   
142 throughout the experiment. Settling particles were quantitatively collected every other day  
143 from sediment traps at the bottom of the mesocosm units and the TPC determined from the  
144 processed samples (Boxhammer et al., 2016) as described above.

145 Mesozooplankton was collected by net hauls (100  $\mu\text{m}$  mesh size), fixed (ethanol) and  
146 counted in a stereomicroscope. Zooplankton carbon biomass (CB) was calculated using the  
147 displacement volume (DV) and the equation of Wiebe (1988):  $(\log DV + 1.429)/0.82 = \log$   
148 CB. Micro and nanoplankton (zoo- and phytoplankton) CB was determined from microscopic  
149 counts of fixed (acidic Lugol's iodine solution) samples, and the cellular bio-volumes were  
150 determined according to Olenina et al. (2006) and converted to POC by the equations  
151 provided by Menden-Deuer and Lessard (2000).

152 Picophytoplankton were counted using flow cytometry and converted to CB by size  
153 fractionation (Veldhuis and Kraay, 2004) and cellular carbon conversion factors ( $0.2 \text{ pg C}$   
154  $\mu\text{m}^{-3}$  (Waterbury et al., 1986). Prokaryotes and viruses were determined according to Marie et  
155 al. (1999) and Brussaard (2004), respectively. All heterotrophic prokaryotes, hereafter termed  
156 bacteria, and viruses were converted to CB assuming  $12.5 \text{ fg C cell}^{-1}$  (Heinänen and  
157 Kuparinen, 1991) and  $0.055 \text{ fg C virus}^{-1}$  (Steward et al., 2007), respectively.

158 The respiration rate was calculated from the difference between the O<sub>2</sub> concentration  
159 (measured with a Fibox 3, PreSens) before and after a 48 h incubation period in a dark,  
160 climate controlled room set to the average temperature observed in the mesocosms.



161 Bacterial protein production (BPP) was determined by  $^{14}\text{C}$ -leucine ( $^{14}\text{C}$ -Leu) incorporation  
162 (Simon and Azam, 1989) according to Grossart et al. (2006). The amount of incorporated  
163  $^{14}\text{C}$ -Leu was converted into BPP by using an intracellular isotope dilution factor of 2. A  
164 conversion factor of 0.86 was used to convert the produced protein into carbon (Simon and  
165 Azam, 1989).

166 Net primary production (NPP) was measured using radio-labeled  $\text{NaH}^{14}\text{CO}_3$  (Steeman-  
167 Nielsen, 1952). Samples were incubated for 24 h in duplicate, 8 ml vials moored on small  
168 incubation platforms at 2, 4, 6, 8 and 10 m depth next to the mesocosms. The areal primary  
169 production was calculated based on a simple linear model of the production measurements  
170 from the different depths (Spilling et al., 2016).

171

### 172 **2.3. Gas exchange**

173 In order to calculate the  $\text{CO}_2$  gas exchange with the atmosphere ( $\text{CO}_{2\text{flux}}$ ), we used  $\text{N}_2\text{O}$  as  
174 tracer gas, and this was added to mesocosm M5 and M8 (control and high  $\text{CO}_2$  treatment)  
175 according to Czerny et al. (2013b). The  $\text{N}_2\text{O}$  concentration was determined every second day  
176 using gas chromatography. Using the  $\text{N}_2\text{O}$  measurements, the fluxes across the water surface  
177 ( $F_{\text{N}_2\text{O}}$ ) was calculated according to:

$$178 \quad F_{\text{N}_2\text{O}} = I_{t_1} - I_{t_2} / (A * \Delta t) \quad (1)$$

179 where  $I_{t_1}$  and  $I_{t_2}$  is the bulk  $\text{N}_2\text{O}$  concentration at time:  $t_1$  and  $t_2$ ;  $A$  is the surface area and  $\Delta t$   
180 is the time difference between  $t_1$  and  $t_2$ .

181 The flux velocity was then calculated by:

$$182 \quad K_{\text{N}_2\text{O}} = F_{\text{N}_2\text{O}} / (C_{\text{N}_2\text{Ow}} - (C_{\text{N}_2\text{Oaw}})) \quad (2)$$

183 where  $C_{\text{N}_2\text{Ow}}$  is the bulk  $\text{N}_2\text{O}$  concentration in the water at a given time point, and  $C_{\text{N}_2\text{Oaw}}$  is  
184 the equilibrium concentration for  $\text{N}_2\text{O}$  (Weiss and Price, 1980).

185 The flux velocity for  $\text{CO}_2$  was calculated from the flux velocity of  $\text{N}_2\text{O}$  according to:

$$186 \quad k_{\text{CO}_2} = k_{\text{N}_2\text{O}} / (S_{\text{C}_{\text{CO}_2}}/S_{\text{C}_{\text{N}_2\text{O}}})^{0.5} \quad (3)$$

187 where  $S_{\text{C}_{\text{CO}_2}}$  and  $S_{\text{C}_{\text{N}_2\text{O}}}$  are the Schmidt numbers for  $\text{CO}_2$  and  $\text{N}_2\text{O}$ , respectively. The  $\text{CO}_2$  flux  
188 across the water surface was calculated according to:

189  $F_{CO_2} = k_{CO_2} (C_{CO_2w} - C_{CO_2aw})$  (4)

190 where  $C_{CO_2w}$  is the water concentration of  $CO_2$  and  $C_{CO_2aw}$  is the equilibrium concentration of  
191  $CO_2$ .  $CO_2$  is preferentially taken up by phytoplankton at the surface, where also the  
192 atmospheric exchange takes place. For this reason, we used the calculated  $CO_2$  concentration  
193 (based on the integrated  $CO_2$  concentration and pH in the surface) from the upper 5 m as the  
194 input for equation 5.

195 In contrast to  $N_2O$ , the  $CO_2$  flux can be chemically enhanced by hydration reactions of  $CO_2$   
196 with hydroxide ions and water molecules in the boundary layer (Wanninkhof and Knox,  
197 1996). Using the method outlined in Czerny et al. (2013b) we found an enhancement of up to  
198 12% on warm days and this was included into our flux calculations.

199

#### 200 **2.4. Data treatment**

201 The primary data generated in this study comprise of carbon standing stock measurements of  
202 TPC, DOC, DIC, as well as carbon estimates of meso- and microzooplankton, micro-, nano-  
203 and picophytoplankton, bacteria and viruses. Flux measurements of atmospheric  $CO_2$   
204 exchange and sedimentation of TPC, as well as the biological rates of net primary production  
205 ( $NPP_{14C}$ ), bacterial production (BP) and total respiration (TR) enabled us to make carbon  
206 budget.

207 Based on the primary variables (Chl *a* and temperature), the experiment where divided into  
208 three distinct phases: Phase I: *t0-t16*; Phase II: *t17-t30* and Phase III: *t31-t43*, where e.g.  
209 Chlorophyll *a* (Chl *a*) concentration was relatively high during Phase I, decreased during  
210 Phase II and remained low during Phase III (Paul et al. 2015). Measurements of pools and  
211 rates were average for the two first sampling points of each experimental phase ( $n = 2$ ) and  
212 where normalized to  $m^2$  knowing the total depth (17 m, excluding the sedimentation funnel)  
213 of the mesocosms. [For Phase III we used the average of the last two measurements as the end](#)  
214 [point \( \$n = 2\$ \).](#)

215 For fluxes and biological rates we used the average for the whole periods normalized to days  
216 ( $day^{-1}$ ). The [same was done for](#) rates of change ( $\Delta TPC$ ,  $\Delta DOC$  and  $\Delta DIC$ ), [which accounted](#)  
217 [for the ~~were the~~](#) difference between the start and end of each phase [for all carbon pools](#)  
218 [\( \$TPC\_{pool}\$ ,  \$DOC\_{pool}\$ ,  \$DIC\_{pool}\$ \). All error estimates were calculated as standard error \(SE\), and](#)  
219 [this was calculated using all measurements within each phase \(e.g. calculating the  \$\Delta TPC\$  SE](#)

Formatted: Subscript

220 [using the difference between each TPC measurement](#)). The three different phases of the  
221 experiments were of different length [and each variable had a slightly different sampling](#)  
222 [regime \(every 1-3 days, and some measurements missing due to technical problems\)](#). The  
223 [exact sample number \(n\) for each SE is presented in the Table legends 1-3. with n = 16, n =](#)  
224 [14 and n = 13 for Phases I—III respectively.](#) The SE for estimated rates were calculated from  
225 the square root of the sum of variance for all the variables (Eq 5-10 below) The primary  
226 papers mentioned above (section 2.2.) present detailed statistical analyses and we only refer  
227 to those here.

228 NPP was measured directly and we additionally estimated the net community production  
229 (NCP). This was done in two different ways from the organic (NCP<sub>o</sub>), dissolved plus  
230 particulate and inorganic (NCP<sub>i</sub>) fractions of carbon. NCP<sub>o</sub> was calculated from changes in  
231 the organic fraction plus the exported TPC (EXP<sub>TPC</sub>) according to:

$$232 \text{NCP}_o = \text{EXP}_{\text{TPC}} + \Delta\text{TPC} + \Delta\text{DOC} \quad (5)$$

233 Direct measurements using <sup>14</sup>C isotope incubations should in principal provide a higher value  
234 than summing up the difference in overall carbon balance (our NCP<sub>o</sub>), as the latter would  
235 incorporate total respiration and not only autotrophic respiration. NCP<sub>i</sub> was calculated  
236 through changes in the dissolved inorganic carbon pool, corrected for CO<sub>2</sub> gas exchange with  
237 the atmosphere (CO<sub>2</sub>flux) according to:

$$238 \text{NCP}_i = \text{CO}_{2\text{flux}} - \Delta\text{DIC} \quad (6)$$

239 In order to close the budget we estimated gross primary production (GPP) and DOC  
240 production (DOC<sub>prod</sub>). GPP is defined as the photosynthetically fixed carbon without any loss  
241 processes (i.e. NPP + autotrophic respiration). GPP can be estimated based on changes in  
242 organic (GPP<sub>o</sub>) or inorganic (GPP<sub>i</sub>) carbon pools, and we used these two different approaches  
243 providing a GPP range:

$$244 \text{GPP}_o = \text{NCP}_o + \text{TR} \quad (7)$$

$$245 \text{GPP}_i = \text{TR} + \text{CO}_{2\text{flux}} - \Delta\text{DIC} \quad (8)$$

246 During Phase III, TR was not measured and we estimated TR based on the ratios  
247 [between](#) NCP<sub>o</sub> and BP to TR during Phase II. The minimum production of DOC  
248 (DOC<sub>minp</sub>) in the system was calculated assuming bacterial carbon uptake was taken from the  
249 DOC pool according to:

250  $DOC_{\min p} = \Delta DOC + BP$  (9)

251 However, this could underestimate  $DOC_{\text{prod}}$  as a fraction of bacterial DOC uptake is respired.  
252 Without direct measurement of (heterotrophic prokaryote) bacterial respiration, (BR), we  
253 estimated BR from TR. The share of active bacteria contributing to bacterial production is  
254 typically in the range of 10-30% of the total bacterial community (Lignell et al., 2013). We  
255 used the fraction of bacterial biomass (BB) of total biomass (TB) as the maximum limit of  
256 BR ( $BR \leq BB/TB$ ), and hence calculated max DOC production ( $DOC_{\text{maxp}}$ ) according to:

257  $DOC_{\text{maxp}} = \Delta DOC + BP + (BB * TR / TB)$  (10)

258 We assumed that carbon synthesized by bacteria added to the TPC pool.

259 There are a number of uncertainties in these calculations, but this budgeting exercise provides  
260 an order-of-magnitude estimate of the flow of carbon within the system and enables  
261 comparison between the treatments. The average of the two controls (M1 and M5) and two  
262 highest CO<sub>2</sub> treatments (M3 and M8) were used to illustrate CO<sub>2</sub> effects.

263

### 264 3. Results and discussion

#### 265 3.1 Change in plankton community, from large to small forms over time

266 The overall size structure of the plankton community decreased over the course of the  
267 experiment. Fig 1 illustrates the carbon content in different plankton groups in the control  
268 mesocosms. During Phase I, the phytoplankton abundances increased at first in all treatments  
269 before starting to decrease at the end of Phase I (Paul et al., 2015). At the start of Phase II  
270 (t17), the phytoplankton biomass was higher than at the start of the experiment (~130 mmol  
271 C m<sup>-2</sup> in the controls) but decreased throughout Phase II and III. The fraction of  
272 picophytoplankton increased in all treatments, but some groups of picophytoplankton  
273 increased more in the high CO<sub>2</sub> treatments (Crawford et al., 2016).

274 Nitrogen was the limiting nutrient throughout the entire experiment (Paul et al., 2015), and  
275 primary producers are generally N-limited in the main sub-basins of the Baltic Sea  
276 (Tamminen and Andersen, 2007). The surface to volume ratio increases with decreasing cell  
277 size, and consequently small cells have higher nutrient affinity, and are better competitors for  
278 scarce nutrient sources than large cells (Reynolds, 2006). The prevailing N-limitation was  
279 likely the reason for the decreasing size structure of the phytoplankton community.

280 Micro and mesozooplankton standing stock was approximately half of the phytoplankton  
281 biomass initially, but decreased rapidly in the control treatments during Phase I (Fig 1). In the  
282 CO<sub>2</sub> enriched treatments the zooplankton biomass also decreased but not to the same extent  
283 as in the control treatments (Spilling et al., 2016). Overall, smaller species benefitted from the  
284 extra CO<sub>2</sub> addition, but there was no significant negative effect of high CO<sub>2</sub> on the  
285 mesozooplankton community (Lischka et al., 2015).

286 Bacterial biomass was the main fraction of the plankton carbon throughout the experiment.  
287 The bacterial numbers largely followed the phytoplankton biomass with an initial increase  
288 then decrease during Phase I; increase during Phase II and slight decrease during Phase III  
289 (Crawfurd et al., 2016). The bacterial community was controlled by mineral nutrient  
290 limitation, bacterial grazing and viral lysis (Crawfurd et al., 2016), and bacterial growth is  
291 typically limited by N or a combination of N and C in the study area (Lignell et al., 2008;  
292 Lignell et al., 2013).

293 The bacterial carbon pool was higher than the measured TPC. Part of the bacteria must have  
294 passed the GFF filters (0.7 µm), and assuming pico- to mesoplankton was part of the TPC,  
295 >50% of the bacterial carbon was not contributing to the measured TPC. The conversion  
296 factor from cells to carbon is positively correlated to cell size, and there is consequently  
297 uncertainty related to the absolute carbon content of the bacterial pool (we used a constant  
298 conversion factor). However, bacteria is known to be the dominating carbon share in the  
299 Baltic Sea during the N-limited summer months (Lignell et al., 2013), and its relative  
300 dominance is in line with this.

301 Although there are some uncertainty in the carbon estimate (Jover et al. 2014), virus make up  
302 (due to their numerical dominance) a significant fraction of the pelagic carbon pool. Of the  
303 different plankton fractions the virioplankton have been the least studied, but their role in the  
304 pelagic ecosystem is ecologically important (Suttle, 2007; Brussaard et al., 2008; Mojica et  
305 al., 2016). Viral lysis rates were equivalent to the grazing rates for phytoplankton and for  
306 bacteria in the current study (Crawfurd et al., 2015). As mortality agents, viruses are key  
307 drivers of the regenerative microbial food web (Suttle, 2007; Brussaard et al., 2008). Overall,  
308 the structure of the plankton community reflected the nutrient status of the system. The  
309 increasing N-limitation favoring development of smaller cells, and increasing dependence of  
310 the primary producers on regenerated nutrients.

311

### 312 **3.2. The DIC pool and atmospheric exchange of CO<sub>2</sub>**

313 The DIC pool was the largest carbon pool: 3-4 fold higher than the DOC pool and roughly  
314 60-fold higher than the TPC pool (Tables 1-3). After the addition of CO<sub>2</sub>, the DIC pool was  
315 ~7% higher in the highest CO<sub>2</sub> treatment compared to the control mesocosms (Table 1). The  
316 gas exchange with the atmosphere was the most apparent flux affected by CO<sub>2</sub> addition  
317 (Tables 1-3). Seawater in the mesocosms with added CO<sub>2</sub> were supersaturated, hence CO<sub>2</sub>  
318 outgassed throughout the experiment. The control mesocosms were initially undersaturated,  
319 hence ingassing occurred during Phases I and II (Fig 2). In the first part of Phase III, the  
320 control mesocosms reached equilibrium with the atmospheric *f*CO<sub>2</sub> (Fig. 2). The gas  
321 exchange had direct effects on the DIC concentration in the mesocosms (Fig. 3). From the  
322 measured gas exchange and change in DIC it is possible to calculate the biologically  
323 mediated carbon flux. In the mesocosms with ambient CO<sub>2</sub> concentration, the flux  
324 measurements indicated net heterotrophy throughout the experiment. The opposite pattern,  
325 net autotrophy, was indicated in the two mesocosms with the highest CO<sub>2</sub> addition (Fig 3; see  
326 also section 3.7.).

327

### 328 **3.3. The DOC pool, DOC production and remineralization**

329 The DOC pool increased throughout the experiment in all mesocosm bags, but more in the  
330 treatments with elevated CO<sub>2</sub> concentration. The initial DOC standing stock in all treatments  
331 was approximately 7200 mmol C m<sup>-2</sup>. At the end of the experiment, the DOC pool was ~2%  
332 higher in the two highest CO<sub>2</sub> treatments compared to the controls (Fig. 4), and there is  
333 statistical support for this difference between CO<sub>2</sub> treatments (Phase III, *p* = 0.05) (Paul et al.,  
334 2015). Interestingly, the data does not point to a substantially higher release of DOC at high  
335 CO<sub>2</sub> (Figs 4 and 5). The bacterial production was notably lower during Phases II and III in  
336 the high CO<sub>2</sub> treatments (Hornick et al., 2016), and of similar magnitude as the rate of change  
337 in DOC pool (Table 2 and 3), indicating reduced bacterial uptake and remineralization of  
338 DOC. The combined results suggest that the increase in the DOC pool at high CO<sub>2</sub> was  
339 related to reduced DOC loss (uptake by bacteria), rather than increased release of DOC by the  
340 plankton community, at elevated CO<sub>2</sub> concentration.

341 The Baltic Sea is affected by large inflow of freshwater containing high concentrations of  
342 refractory DOC such as humic substances, and the concentration in Gulf of Finland is  
343 typically 400-500 μmol C L<sup>-1</sup> (Hoikkala et al., 2015). The large pool of DOC and turn over

344 times of ~200 days (Tables 1-3) is most likely a reflection of the relatively low fraction of  
345 labile DOC, but bacterial limitation of mineral nutrients can also increase turn over times  
346 (Thingstad et al., 1997).

347 The DOC pool has been demonstrated to aggregate into transparent exopolymeric particles  
348 (TEP) under certain circumstances, which can increase sedimentation at high CO<sub>2</sub> levels  
349 (Riebesell et al., 2007). We did not have any direct measurements of TEP, but any CO<sub>2</sub> effect  
350 on its formation is highly dependent on the plankton community and its physiological status  
351 (MacGilchrist et al., 2014). No observed effect of CO<sub>2</sub> treatment on carbon export suggests  
352 that we did not have a community where the TEP production was any different between the  
353 treatments used.

354

### 355 **3.4. The TPC pool and export of carbon**

356 There was a positive effect of elevated CO<sub>2</sub> on TPC relative to the controls. At the start of the  
357 experiment, the measured TPC concentration in the enclosed water columns was 400-500  
358 mmol C m<sup>-2</sup> (Table 1). The TPC pool decreased over time but less in the high CO<sub>2</sub> treatment  
359 and at the end of the experiment, the standing stock of TPC was ~6% higher (Phase III, p =  
360 0.01; Paul et al. (2015) in the high CO<sub>2</sub> treatment (Fig. 4).

361 The export of TPC was not dependent on the CO<sub>2</sub> concentration but varied temporally. The  
362 largest flux of TPC out of the mesocosms occurred during Phase I with ~6 mmol C m<sup>-2</sup> d<sup>-1</sup>. It  
363 decreased to ~3 mmol C m<sup>-2</sup> d<sup>-1</sup> during Phase II and was ~2 mmol C m<sup>-2</sup> d<sup>-1</sup> during Phase III  
364 (Table 1-3). The exported carbon as percent of average TPC standing stock similarly  
365 decreased from ~1.3% during Phase I to 0.3-0.5% during Phase III. The initial increase in the  
366 autotrophic biomass was the likely reason for relatively more of the carbon settling in the  
367 mesocosms in the beginning of the experiment whereas the decreasing carbon export was  
368 most likely caused by the shift towards a plankton community depending on recycled  
369 nitrogen. This reduced the overall suspended TPC and also the average plankton size in the  
370 community.

371

### 372 **3.5. Biological rates: respiration**

373 Total respiration (TR) was always lower in the CO<sub>2</sub> enriched treatments (Tables 1-3). The  
374 average TR was 83 mmol C m<sup>-2</sup> d<sup>-1</sup> during Phase I, and initially without any detectable

375 treatment effect. The respiration rate started to be lower in the high CO<sub>2</sub> treatments,  
376 compared with the controls, in the beginning of Phase II. At the end of Phase II there was a  
377 significant difference ( $p = 0.02$ ; Spilling et al., 2016) between the treatments (Table 2), and  
378 40% lower respiration rate in the highest CO<sub>2</sub> treatment compared with the controls (Spilling  
379 et al., 2016).

380 Cytosol pH is close to neutral in most organisms, and reduced energetic cost for internal pH  
381 regulation (e.g. transport of H<sup>+</sup>) and at lower external pH levels could be one factor reducing  
382 respiration (Smith and Raven, 1979). Hopkinson et al. (2010) found indirect evidence for  
383 decreased respiration and also proposed that increased CO<sub>2</sub> concentration (i.e. decreased pH)  
384 reduced metabolic cost of remaining intracellular homeostasis. Mitochondrial respiration in  
385 plant foliage decreases in high CO<sub>2</sub> environments, possibly affected by respiratory enzymes  
386 or other metabolic processes (Amthor, 1991; Puhe and Ulrich, 2012). Most inorganic carbon  
387 in water is in the form of bicarbonate (HCO<sub>3</sub><sup>-</sup>) at relevant pH, and many aquatic autotrophs  
388 have developed carbon concentrating mechanisms (CCMs) (e.g. Singh et al., 2014) that could  
389 reduce the cost of growth (Raven, 1991). There are some studies that have pointed to savings  
390 of metabolic energy due to down-regulation of carbon concentrating mechanisms (Hopkinson  
391 et al., 2010) or overall photosynthetic apparatus (Sobrino et al., 2014) in phytoplankton at  
392 high CO<sub>2</sub> concentrations. Yet, other studies of the total plankton community have pointed at  
393 no effect or increased respiration at elevated CO<sub>2</sub> concentration (Li and Gao, 2012; Tanaka et  
394 al., 2013), and the metabolic changes behind reduced respiration, remains an open question.  
395 Membrane transport of H<sup>+</sup> is sensitive to changes in external pH, but the physiological  
396 impacts of increasing H<sup>+</sup> needs further study to better address effects of ocean acidification  
397 (Taylor et al., 2012). An important aspect is also to consider the microenvironment  
398 surrounding plankton; exchange of nutrients and gases takes place through the boundary  
399 layer, which might have very different pH properties than bulk water measurements (Flynn et  
400 al., 2012).

401

### 402 **3.6. Biological rates: bacterial production**

403 Bacterial production (BP) became lower in the high CO<sub>2</sub> treatment in the latter part of the  
404 experiment. During Phase I, BP ranged from 27 to 46 mmol C m<sup>-2</sup> d<sup>-1</sup> (Table 1). The  
405 difference in BP between treatments became apparent in Phases II and III of the experiment.  
406 The average BP was 18% and 24% higher in the controls compared to the highest CO<sub>2</sub>



407 treatments during Phases II and III, respectively (Tables 2 and 3). Statistical support ( $p \leq 0.01$ )  
408 for a treatment effect during parts of the experiment is presented in Hornick et al. (2016).

409 The lower bacterial production accounted for ~40% of the reduced respiration during Phase  
410 II, and the reduced respiration described above could at least partly be explained by the lower  
411 bacterial activity. This raises an interesting question: what was the mechanism behind the  
412 reduced bacterial production/respiration in the high CO<sub>2</sub> treatment? There are examples of  
413 decreased bacterial production (Motegi et al 2013) and respiration (Teira et al., 2012) at  
414 elevated CO<sub>2</sub> concentration. However, most previous studies have reported no change  
415 (Allgaier et al., 2008) or a higher bacterial production at elevated CO<sub>2</sub> concentration  
416 (Grossart et al., 2006; Piontek et al., 2010; Endres et al., 2014). The latter was also supported  
417 by the recent study of Bunse et al. (2016), describing up-regulation of bacterial genes related  
418 to respiration, membrane transport and protein metabolism at elevated CO<sub>2</sub> concentration;  
419 albeit, this effect was not evident when inorganic nutrients had been added (high Chl *a*  
420 treatment).

421 In this study, the reason for the lower bacterial activity in the high CO<sub>2</sub> treatments could be  
422 due to either limitation and/or inhibition of bacterial growth or driven by difference in loss  
423 processes. Bacterial grazing and viral lysis was higher in the high CO<sub>2</sub> treatments during  
424 periods of the experiment (Crawford et al., 2016), and would at least partly be the reason for  
425 the reduced bacterial production at high CO<sub>2</sub> concentration.

426 N-limitation increased during the experiment (Paul et al., 2015), and mineral nutrient  
427 limitation of bacteria can lead to accumulation of DOC, i.e. reduced bacterial uptake  
428 (Thingstad et al., 1997), similar to our results. Bacterial N limitation is common in the area  
429 during summer (Lignell et al., 2013), however, this N-limitation was not apparently different  
430 in the controls (Paul et al., 2015), and CO<sub>2</sub> did not affect N-fixation (Paul et al., 2016). In a  
431 scenario where the competition for N is fierce, the balance between bacteria and similar sized  
432 picophytoplankton could be tilted in favor of phytoplankton if they gain an advantage by  
433 having easier access to carbon, i.e. CO<sub>2</sub> (Hornick et al., 2016). We have not found evidence  
434 in the literature that bacterial production will be suppressed in the observed pH range inside  
435 the mesocosms, varying from approximately pH 8.1 in the control to pH 7.6 in the highest  
436 *f*CO<sub>2</sub> treatment (Paul et al., 2015), although enzyme activity seems to be affected even by  
437 moderate pH changes. For example, some studies report on an increase in protein degrading  
438 enzyme leucine aminopeptidase activities at reduced pH (Grossart et al., 2006; Piontek et al.,  
439 2010; Endres et al., 2014), whereas others indicate a reduced activity of this enzyme

440 (Yamada and Suzumura, 2010). A range of other factors affects this enzyme, for example the  
441 nitrogen source and salinity (Stepanauskas et al., 1999), and any potential interaction effects  
442 with decreasing pH are not yet resolved. Any pH-induced changes in bacterial enzymatic  
443 activity could potentially affect bacterial production.

444

### 445 **3.7. Biological rates: primary production**

446 There was an effect of CO<sub>2</sub> concentration on the net community production based on the  
447 organic carbon fraction (NCP<sub>o</sub>). NCP<sub>o</sub> was higher during Phase I than during the rest of the  
448 experiments and during this initial phase without any apparent CO<sub>2</sub> effect. There was no  
449 consistent difference between CO<sub>2</sub> treatments for NPP<sub>14C</sub> ( $p > 0.1$ ), but NCP<sub>o</sub> increased with  
450 increasing CO<sub>2</sub> enrichment during Phase II (Phase II; linear regression  $p = 0.003$ ;  $R^2 = 0.91$ ).  
451 This was caused by the different development in the TPC and DOC pools. The pattern of  
452 gross primary production (GPP) was similar to NCP<sub>o</sub> during Phases I and II. During Phase III  
453 there were no respiration or NPP<sub>14C</sub> measurements and the estimated GPP is more uncertain.  
454 The NCP<sub>o</sub> and GPP indicated a smaller difference between treatments during Phase III  
455 compared with Phase II.

456 The measures of NPP<sub>14C</sub> and NCP<sub>o</sub> were of a similar magnitude (Tables 1-3). During Phase I,  
457 NPP<sub>14C</sub> < NCP<sub>o</sub> (Table 1), this relationship reversed for most treatments during Phase II, with  
458 the exception of the highest CO<sub>2</sub> levels (Table 2). The difference between NPP<sub>14C</sub> and NCP<sub>o</sub>  
459 suggests that observed reduction in respiration at elevated CO<sub>2</sub> could be mainly heterotrophic  
460 respiration. However, in terms of the NPP<sub>14C</sub> < NCP<sub>o</sub>, the uncertainty seems to be higher than  
461 the potential signal of heterotrophic respiration. This would also indicate that the NPP<sub>14C</sub>  
462 during Phase I have been underestimated, in particular for the control mesocosm M1. During  
463 Phase II, the NPP<sub>14C</sub> was higher than NCP<sub>o</sub>, except for the two highest CO<sub>2</sub> treatments, more  
464 in line with our assumption of NPP<sub>14C</sub> > NCP<sub>o</sub>. The systematic offset in NPP<sub>14C</sub> during Phase  
465 I could be due to changed parameterization during incubation in small volumes (8 mL,  
466 Spilling et al., 2016), for example increased loss due to grazing.

467 The results of the DIC pool and atmospheric exchange of CO<sub>2</sub> provides another way of  
468 estimating the net community production based on inorganic carbon (NCP<sub>i</sub>). There was some  
469 discrepancy between the NCP<sub>o</sub> and NCP<sub>i</sub> as the latter suggested net heterotrophy in the  
470 ambient CO<sub>2</sub> whereas the high CO<sub>2</sub> treatments were net autotrophic during all three phases of  
471 the experiment (Fig. 3). For the NCP<sub>o</sub> there was no indication of net heterotrophy at ambient

472 CO<sub>2</sub> concentration. In terms of the absolute numbers, the NCP<sub>i</sub> estimate is probably more  
473 uncertain than NCP<sub>o</sub>. Calculating the CO<sub>2</sub> atmospheric exchange from the measurements of a  
474 tracer gas involves several calculation steps (Eq 1-4), each adding uncertainty to the  
475 calculation. However, both estimations (NCP<sub>i</sub> and NCP<sub>o</sub>) indicate that increased CO<sub>2</sub>  
476 concentrations lead to higher overall community production, supporting our overall  
477 conclusion.

478

479

### 480 **3.8 Budget**

481 A carbon budget for the two control mesocosms and two highest CO<sub>2</sub> additions is presented  
482 in Fig. 5. During Phase I the estimated gross primary production (GPP) was ~100 mmol C  
483 fixed m<sup>-2</sup> d<sup>-1</sup>; from which 75-95% were respired, ~1% ended up in the TPC (including export)  
484 and 5-25% added to the DOC pool. The main difference between CO<sub>2</sub> treatments became  
485 apparent during Phase II when the NCP<sub>o</sub> was higher in the elevated CO<sub>2</sub> treatments. The  
486 respiration loss increased to ~100% of GPP at the ambient CO<sub>2</sub> concentration, whereas  
487 respiration was lower (85-95% of GPP) in the highest CO<sub>2</sub> treatment. Bacterial production  
488 was ~30% lower, on average, at the highest CO<sub>2</sub> concentration compared with the controls  
489 during Phase II. The share of NCP<sub>o</sub> of GPP ranged from 2% to 20% and the minimum flux to  
490 the DOC pool was 11% to 18% of TPC.

491 The overall budget was calculated by using the direct measurements of changes in standing  
492 stocks and fluxes of export, respiration and bacterial production rates. The most robust data  
493 are the direct measurements of carbon standing stocks and their development (e.g. ΔTPC).  
494 These are based on well-established analytical methods with relatively low standard error  
495 (SE) of the carbon pools. However, the dynamic nature of these pools made the relative SE  
496 for the rate of change much higher, reflecting that the rate of change varied considerably  
497 within the different phases.

498 The rate [variablesparameters](#), calculated based on conversion factors, have greater  
499 uncertainty, although their SEs were relatively low, caused by uncertainty in the conversion  
500 steps. For example, the respiratory quotient (RQ) was set to one, which is a good estimate for  
501 carbohydrate oxidation. For lipids and proteins the RQ is close to 0.7, but in a natural  
502 environment RQ is often >1 (Berggren et al., 2012), and is affected by physiological state e.g.  
503 nutrient limitation (Romero-Kutzner et al., 2015). Any temporal variability in the conversion

504 factors would directly change the overall budget calculations, e.g. RQ affecting total  
505 respiration and gross primary production estimates. However, the budget provides an order-  
506 of-magnitude estimate of the carbon flow within the system. Some of the [variablesparameters](#)  
507 such as GPP were estimated using different approaches, providing a more robust comparison  
508 of the different treatments.

509 The primary effect of increasing CO<sub>2</sub> concentration was the higher standing stocks of TPC  
510 and DOC compared with ambient CO<sub>2</sub> concentration. The increasing DOC pool and  
511 relatively higher TPC pool were driven by reduced respiration and bacterial production at  
512 elevated CO<sub>2</sub> concentration. Decreasing respiration rate reduced the recycling of organic  
513 carbon back to the DIC pool. The lower respiration and bacterial production also indicates  
514 reduced remineralization of DOC. These two effects caused the higher TPC and DOC pools  
515 in the elevated CO<sub>2</sub> treatments. The results highlight the importance of looking beyond net  
516 changes in carbon standing stocks to understand how carbon fluxes are affected under  
517 increasing ocean acidification.

518

519

## 520 **Acknowledgements**

521 We would like to thank all of the staff at Tvärminne Zoological station, for great help during  
522 this experiment, and Michael Sswat for carrying out the TPC filtrations. We also gratefully  
523 acknowledge the captain and crew of R/V ALKOR (AL394 and AL397) for their work  
524 transporting, deploying and recovering the mesocosms. The collaborative mesocosm  
525 campaign was funded by BMBF projects BIOACID II (FKZ 03F06550) and SOPRAN Phase  
526 II (FKZ 03F0611). Additional financial support for this study came from Academy of Finland  
527 (KS - Decisions no: 259164 and 263862) and Walter and Andrée de Nottbeck Foundation  
528 (KS). TH and HPG were financially supported by SAW project TemBi of the Leibniz  
529 Foundation. CPDB was financially supported by the Darwin project, the Royal Netherlands  
530 Institute for Sea Research (NIOZ), and the EU project MESOAQUA (grant agreement  
531 number 228224).

532

533

534 **References**

- 535 Allgaier, M., Riebesell, U., Vogt, M., Thyrrhaug, R., and Grossart, H.-P.: Coupling of  
536 heterotrophic bacteria to phytoplankton bloom development at different pCO<sub>2</sub> levels: a  
537 mesocosm study, *Biogeosciences*, 5, 1007-1022, 2008.
- 538 Amthor, J.: Respiration in a future, higher-CO<sub>2</sub> world, *Plant, Cell & Environment*, 14, 13-20,  
539 1991.
- 540 Badr, E.-S. A., Achterberg, E. P., Tappin, A. D., Hill, S. J., and Braungardt, C. B.:  
541 Determination of dissolved organic nitrogen in natural waters using high temperature  
542 catalytic oxidation, *Trends in Analytical Chemistry*, 22, 819-827, 2003.
- 543 Berggren, M., Lapierre, J.-F., and del Giorgio, P. A.: Magnitude and regulation of  
544 bacterioplankton respiratory quotient across freshwater environmental gradients, *The*  
545 *ISME journal*, 6, 984-993, 2012.
- 546 Bermúdez, R., Winder, M., Stühr, A., Almén, A.-K., Engström-Öst, J., and Riebesell, U.:  
547 Effect of ocean acidification on the structure and fatty acid composition of a natural  
548 plankton community in the Baltic Sea, *Biogeosciences Discuss*, 10.5194/bg-2015-669,  
549 2016.
- 550 Boxhammer, T., Bach, L. T., Czerny, J., and Riebesell, U.: Technical Note: Sampling and  
551 processing of mesocosm sediment trap material for quantitative biogeochemical  
552 analyses, *Biogeosciences Discuss*, 13, 2849-2858, 2016.
- 553 Brussaard, C. P.: Optimization of procedures for counting viruses by flow cytometry, *Appl*  
554 *Env Microbiol*, 70, 1506-1513, 2004.
- 555 Brussaard, C., Wilhelm, S. W., Thingstad, F., Weinbauer, M. G., Bratbak, G., Heldal, M.,  
556 Kimmance, S. A., Middelboe, M., Nagasaki, K., and Paul, J. H.: Global-scale processes  
557 with a nanoscale drive: the role of marine viruses, *Isme Journal*, 2, 575, 2008.
- 558 Bunse, C., Lundin, D., Karlsson, C. M., Vila-Costa, M., Palovaara, J., Akram, N., Svensson,  
559 L., Holmfeldt, K., González, J. M., and Calvo, E.: Response of marine bacterioplankton  
560 pH homeostasis gene expression to elevated CO<sub>2</sub>, *Nature Clim Change*, 2016.
- 561 Crawford, K. J., Riebesell, U., and Brussaard, C. P. D.: Shifts in the microbial community in  
562 the Baltic Sea with increasing CO<sub>2</sub> *Biogeosciences Discuss*, 10.5194/bg2015-606,  
563 2016.
- 564 Czerny, J., Schulz, K. G., Boxhammer, T., Bellerby, R., Büdenbender, J., Engel, A., Krug, S.  
565 A., Ludwig, A., Nachtigall, K., and Nondal, G.: Implications of elevated CO<sub>2</sub> on

566 pelagic carbon fluxes in an Arctic mesocosm study - an elemental mass balance  
567 approach, *Biogeosciences*, 10, 3109–3125, 10.5194/bg-10-3109-2013, 2013a.

568 Czerny, J., Schulz, K. G., Ludwig, A., and Riebesell, U.: A simple method for air/sea gas  
569 exchange measurement in mesocosms and its application in carbon budgeting,  
570 *Biogeosciences*, 10, 1379-1390, 2013b.

571 De Kluijver, A., Soetaert, K., Schulz, K. G., Riebesell, U., Bellerby, R., and Middelburg, J.:  
572 Phytoplankton-bacteria coupling under elevated CO<sub>2</sub> levels: a stable isotope labelling  
573 study, *Biogeosciences*, 7, 3783-3797, 2010.

574 Egge, J., Thingstad, J., Larsen, A., Engel, A., Wohlers, J., Bellerby, R., and Riebesell, U.:  
575 Primary production during nutrient-induced blooms at elevated CO<sub>2</sub> concentrations,  
576 *Biogeosciences*, 6, 877-885, 2009.

577 Endres, S., Galgani, L., Riebesell, U., Schulz, K.-G., and Engel, A.: Stimulated bacterial  
578 growth under elevated pCO<sub>2</sub>: results from an off-shore mesocosm study, *Plos One*, 9,  
579 e99228, 10.1371/journal.pone.0099228, 2014.

580 Engel, A., Borchard, C., Piontek, J., Schulz, K. G., Riebesell, U., and Bellerby, R.: CO<sub>2</sub>  
581 increases <sup>14</sup>C-primary production in an Arctic plankton community, *Biogeosciences*,  
582 10, 1291-1308, 2013.

583 Flynn, K. J., Blackford, J. C., Baird, M. E., Raven, J. A., Clark, D. R., Beardall, J., Brownlee,  
584 C., Fabian, H., and Wheeler, G. L.: Changes in pH at the exterior surface of plankton with  
585 ocean acidification, *Nature Clim Change*, 2, 510-513, 2012.

586 Grossart, H.-P., Allgaier, M., Passow, U., and Riebesell, U.: Testing the effect of CO<sub>2</sub>  
587 concentration on the dynamics of marine heterotrophic bacterioplankton, *Limnol*  
588 *Oceanogr*, 51, 1-11, 2006.

589 Heinänen, A., and Kuparinen, J.: Horizontal variation of bacterioplankton in the Baltic Sea,  
590 *Appl Env Microbiol*, 57, 3150-3155, 1991.

591 Hoikkala, L., Kortelainen, P., Soinne, H., and Kuosa, H.: Dissolved organic matter in the  
592 Baltic Sea, *J Mar Sys*, 142, 47-61, 2015.

593 Hopkinson, B. M., Xu, Y., Shi, D., McGinn, P. J., and Morel, F. M.: The effect of CO<sub>2</sub> on the  
594 photosynthetic physiology of phytoplankton in the Gulf of Alaska, *Limnol Oceanogr*,  
595 55, 2011-2024, 2010.

596 Hornick, T., Bach, L. T., Crawford, K. J., Spilling, K., Achterberg, E. P., Brussaard, C.,  
597 Riebesell, U., and Grossart, H.-P.: Ocean acidification indirectly alters trophic  
598 interaction of heterotrophic bacteria at low nutrient conditions, *Biogeosciences*  
599 *Discuss*, doi:10.5194/bg-2016-61, 2016.

600 Jover, L. F., Effler, T. C., Buchan, A., Wilhelm, S. W., and Weitz, J. S.: The elemental  
601 composition of virus particles: implications for marine biogeochemical cycles, *Nature*  
602 *Reviews Microbiology*, 12, 519-528, 2014.

603 Le Quéré, C., Raupach, M. R., Canadell, J. G., Marland, G., Bopp, L., Ciais, P., Conway, T.  
604 J., Doney, S. C., Feely, R. A., and Foster, P.: Trends in the sources and sinks of carbon  
605 dioxide, *Nature Geosci*, 2, 831-836, 2009.

606 Li, W., and Gao, K.: A marine secondary producer respire and feeds more in a high CO<sub>2</sub>  
607 ocean, *Marine pollution bulletin*, 64, 699-703, 2012.

608 Lignell, R., Hoikkala, L., and Lahtinen, T.: Effects of inorganic nutrients, glucose and solar  
609 radiation on bacterial growth and exploitation of dissolved organic carbon and nitrogen  
610 in the northern Baltic Sea, *Aquat Microb Ecol*, 51, 209-221, 2008.

611 Lignell, R., Haario, H., Laine, M., and Thingstad, T. F.: Getting the “right” parameter values  
612 for models of the pelagic microbial food web, *Limnol Oceanogr*, 58, 301-313, 2013.

613 Lischka, S., Bach, L. T., Schulz, K.-G., and Riebesell, U.: Micro- and mesozooplankton  
614 community response to increasing levels of *f*CO<sub>2</sub> in the Baltic Sea: insights from a  
615 large-scale mesocosm experiment, *Biogeosciences Discuss*, 10.5194/bgd-12-20025-  
616 2015, 2015.

617 MacGilchrist, G., Shi, T., Tyrrell, T., Richier, S., Moore, C., Dumousseaud, C., and  
618 Achterberg, E. P.: Effect of enhanced pCO<sub>2</sub> levels on the production of dissolved  
619 organic carbon and transparent exopolymer particles in short-term bioassay  
620 experiments, *Biogeosciences*, 11, 3695-3706, 2014.

621 Marie, D., Brussaard, C. P., Thyrhaug, R., Bratbak, G., and Vaultot, D.: Enumeration of  
622 marine viruses in culture and natural samples by flow cytometry, *Appl Env Microbiol*,  
623 65, 45-52, 1999.

624 Menden-Deuer, S., and Lessard, E. J.: Carbon to volume relationships for dinoflagellates,  
625 diatoms, and other protist plankton, *Limnol Oceanogr*, 45, 569-579, 2000.

626 Mojica, K. D., Huisman, J., Wilhelm, S. W., and Brussaard, C. P.: Latitudinal variation in  
627 virus-induced mortality of phytoplankton across the North Atlantic Ocean, *The ISME*  
628 *journal*, 10, 500-513, 2016.

629 Motegi, C., Tanaka, T., Piontek, J., Brussaard, C., Gattuso, J., and Weinbauer, M.: Effect of  
630 CO<sub>2</sub> enrichment on bacterial metabolism in an Arctic fjord, *Biogeosciences*, 10, 3285-  
631 3296, 2013.

632 Niiranen, S., Yletyinen, J., Tomczak, M. T., Blenckner, T., Hjerne, O., MacKenzie, B. R.,  
633 Müller-Karulis, B., Neumann, T., and Meier, H.: Combined effects of global climate

634 change and regional ecosystem drivers on an exploited marine food web, *Global*  
635 *Change Biol*, 19, 3327-3342, 2013.

636 Olenina, I., Hajdu, S., Edler, L., Andersson, A., Wasmund, N., Busch, S., Göbel, J., Gromisz,  
637 S., Huseby, S., Huttunen, M., Jaanus, A., Kokkonen, P., Ledaine, I., and Niemkiewicz,  
638 E.: Biovolumes and size-classes of phytoplankton in the Baltic Sea, *Balt. Sea Environ.*  
639 *Proc.*, HELCOM, 144 pp., 2006.

640 Paul, A. J., Achterberg, E. P., Bach, L. T., Boxhammer, T., Czerny, J., Haunost, M., Schulz,  
641 K.-G., Stühr, A., and Riebesell, U.: No observed effect of ocean acidification on  
642 nitrogen biogeochemistry in a summer Baltic Sea plankton community, *Biogeosciences*  
643 13, 3901-3913, doi:10.5194/bg-13-3901-2016, 2016.

644 Paul, A. J., Bach, L. T., Schulz, K.-G., Boxhammer, T., Czerny, J., Achterberg, E. P.,  
645 Hellemann, D., Trense, Y., Nausch, M., Sswat, M., and Riebesell, U.: Effect of elevated  
646 CO<sub>2</sub> on organic matter pools and fluxes in a summer Baltic Sea plankton community  
647 *Biogeosciences*, 12, 6181-6203, doi:10.5194/bg-12-6181-2015, 2015.

648 Piontek, J., Lunau, M., Handel, N., Borchard, C., Wurst, M., and Engel, A.: Acidification  
649 increases microbial polysaccharide degradation in the ocean, *Biogeosciences*, 7, 1615–  
650 1624, 10.5194/bg-7-1615-2010, 2010.

651 Puhe, J., and Ulrich, B.: *Global climate change and human impacts on forest ecosystems:*  
652 *postglacial development, present situation and future trends in Central Europe,*  
653 *Ecological studies – analysis and synthesis*, Springer, Berlin, 476 pp., 2012.

654 Raven, J. A.: Physiology of inorganic C acquisition and implications for resource use  
655 efficiency by marine phytoplankton: relation to increased CO<sub>2</sub> and temperature, *Plant Cell*  
656 *Environ* 14, 779-794, 1991.

657 Reynolds, C. S.: *Ecology of phytoplankton*, Cambridge University Press, Cambridge, 535  
658 pp., 2006.

659 Riebesell, U., Schulz, K. G., Bellerby, R., Botros, M., Fritsche, P., Meyerhöfer, M., Neill, C.,  
660 Nondal, G., Oschlies, A., and Wohlers, J.: Enhanced biological carbon consumption in  
661 a high CO<sub>2</sub> ocean, *Nature*, 450, 545-548, 2007.

662 Riebesell, U., Achterberg, E., Brussaard, C., Engström-Öst, J., Gattuso, J-P., Grossart, H-P.,  
663 Schulz, K. (Eds): *Effects of rising CO<sub>2</sub> on a Baltic Sea plankton community: ecological*  
664 *and biogeochemical impacts. Special issue in Biogeosciences*, 2015.

665 Romero-Kutzner, V., Packard, T., Berdalet, E., Roy, S., Gagné, J., and Gómez, M.:  
666 *Respiration quotient variability: bacterial evidence*, *Mar Ecol Prog Ser*, 519, 47-59,  
667 2015.



668 Simon, M., and Azam, F.: Protein content and protein synthesis rates of planktonic marine  
669 bacteria, *Mar Ecol Prog Ser*, 51, 201-213, 1989.

670 Singh, S. K., Sundaram, S., and Kishor, K.: *Photosynthetic microorganisms: Mechanism for*  
671 *carbon concentration*, Springer, Berlin, 131 pp., 2014.

672 Smith, F., and Raven, J. A.: Intracellular pH and its regulation, *Ann. Rev. Plant Physiol.*, 30,  
673 289-311, 1979.

674 Sobrino, C., Segovia, M., Neale, P., Mercado, J., García-Gómez, C., Kulk, G., Lorenzo, M.,  
675 Camarena, T., van de Poll, W., Spilling, K., and Ruan, Z.: Effect of CO<sub>2</sub>, nutrients and  
676 light on coastal plankton. IV. Physiological responses, *Aquat Biol*, 22, 77-93, 2014.

677 Spilling, K., Paul, A. J., Virkkala, N., Hastings, T., Lischka, S., Stuhr, A., Bermudez, R.,  
678 Czerny, J., Boxhammer, T., Schulz, K. G., Ludwig, A., and Riebesell, U.: Ocean  
679 acidification decreases plankton respiration: evidence from a mesocosm experiment,  
680 *Biogeosciences Discuss*, in review, 10.5194/bg-2015-608, 2016.

681 Steeman-Nielsen, E.: The use of radioactive carbon for measuring organic production in the  
682 sea, *J. Cons. Int. Explor. Mer.*, 18, 117-140, 1952.

683 Stepanauskas, R., Edling, H., and Tranvik, L. J.: Differential dissolved organic nitrogen  
684 availability and bacterial aminopeptidase activity in limnic and marine waters, *Microb*  
685 *Ecol*, 38, 264-272, 1999.

686 Steward, G. F., Fandino, L. B., Hollibaugh, J. T., Whitley, T. E., and Azam, F.: Microbial  
687 biomass and viral infections of heterotrophic prokaryotes in the sub-surface layer of the  
688 central Arctic Ocean, *Deep Sea Res Pt I*, 54, 1744-1757, 2007.

689 Suttle, C. A.: Marine viruses—major players in the global ecosystem, *Nature Reviews*  
690 *Microbiology*, 5, 801-812, 2007.

691 Tamminen, T., and Andersen, T.: Seasonal phytoplankton nutrient limitation patterns as  
692 revealed by bioassays over Baltic Sea gradients of salinity and eutrophication, *Mar Ecol*  
693 *Prog Ser*, 340, 121-138, 2007.

694 Tanaka, T., Alliouane, S., Bellerby, R., Czerny, J., De Kluijver, A., Riebesell, U., Schulz, K.  
695 G., Silyakova, A., and Gattuso, J.-P.: Effect of increased pCO<sub>2</sub> on the planktonic  
696 metabolic balance during a mesocosm experiment in an Arctic fjord, *Biogeosciences*,  
697 10, 315-325, 2013.

698 Taylor, A. R., Brownlee, C., and Wheeler, G. L.: Proton channels in algae: reasons to be  
699 excited, *Trends Plant Sci*, 17, 675-684, 2012.

700 Teira E., Fernández A., Álvarez-Salgado X. A., García-Martín E. E., Serret P., Sobrino C.:  
701 Response of two marine bacterial isolates to high CO<sub>2</sub> concentration. *Mar Ecol Prog*

702 Ser, 453, 27-36, 2012. Thingstad, T. F., Hagström, Å., and Rassoulzadegan, F.:  
703 Accumulation of degradable DOC in surface waters: Is it caused by a malfunctioning  
704 microbial loop?, *Limnol Oceanogr*, 42, 398-404, 1997.

705 Wanninkhof, R., and Knox, M.: Chemical enhancement of CO<sub>2</sub> exchange in natural waters,  
706 *Limnol Oceanogr*, 41, 689-697, 1996.

707 Waterbury, J. B., Watson, S. W., Valois, F. W., and Franks, D. G.: Biological and ecological  
708 characterization of the marine unicellular cyanobacterium *Synechococcus*, *Can Bull*  
709 *Fish Aquat Sci*, 214, 120, 1986.

710 Weiss, R., and Price, B.: Nitrous oxide solubility in water and seawater, *Mar Chem*, 8, 347-  
711 359, 1980.

712 Veldhuis, M. J., and Kraay, G. W.: Phytoplankton in the subtropical Atlantic Ocean: towards  
713 a better assessment of biomass and composition, *Deep Sea Res Pt I*, 51, 507-530, 2004.

714 Wiebe, P. H.: Functional regression equations for zooplankton displacement volume, wet  
715 weight, dry weight, and carbon: a correction, *Fish. Bull.*, 86, 833-835, 1988.

716 Yamada, N., and Suzumura, M.: Effects of seawater acidification on hydrolytic enzyme  
717 activities, *J Oceanogr*, 66, 233-241, 2010.

718

719

1

2 Table 1. The standing stock of total particulate carbon (TPC<sub>pool</sub>), dissolved organic carbon (DOC<sub>pool</sub>) and dissolved inorganic carbon (DIC<sub>pool</sub>) at the start of  
 3 Phase I in mmol C m<sup>-2</sup> ± SE (n = 2). The DOC<sub>pool</sub> was missing some initial measurements and is the average for all mesocosms assuming that the DOC  
 4 concentration was similar at the onset of the experiment. The net change in TPC (ΔTPC), DOC (ΔDOC) and DIC (ΔDIC) are average changes in the standing  
 5 stocks during Phase I in mmol C m<sup>-2</sup> d<sup>-1</sup> ± SE (n = 28). Flux measurements of atmospheric gas exchange (CO<sub>2flux</sub>) and exported carbon (EXP<sub>TPC</sub>) plus  
 6 biological rates: total respiration (TR), bacterial (BP) and net primary production (NPP<sub>14C</sub>) and net community production estimated based on organic carbon  
 7 pools (NCP<sub>o</sub>) net primary production, are all average for the whole Phase I in mmol C m<sup>-2</sup> d<sup>-1</sup> ± SE (n = ~~4~~13, 9, 16, 7 and 11 for CO<sub>2flux</sub>, EXP<sub>TPC</sub>, TR, BP and  
 8 NPP<sub>14C</sub> respectively). SE for NCP<sub>o</sub> was calculated from the square root of the sum of variance of the three variables used in Eq 6. The NCP<sub>o</sub> was calculated  
 9 from the net change in carbon pools plus carbon export, whereas NPP<sub>14C</sub> was measured carbon fixation using radiolabeled <sup>14</sup>C over a 24 h incubation period *in*  
 10 *situ*. TR was measured as O<sub>2</sub> consumption and for comparison with carbon fixation we used a respiratory quotient (RQ) of 1. CO<sub>2flux</sub> was only calculated for  
 11 the period after full addition of CO<sub>2</sub> (4-16). A total budget of carbon fluxes for ambient and high CO<sub>2</sub> treatments is presented in Fig 5.

12

13 **Phase I (t0-t16)**14 **CO<sub>2</sub> treatment (μatm fCO<sub>2</sub>)****365****368****497****821****1007****1231**15 **Mesocosm number****M1****M5****M7****M6****M3****M8**16 TPC<sub>pool</sub>

417 ± 38

425 ± 39

472 ± 48

458 ± 38

431 ± 48

446 ± 57

17 DOC<sub>pool</sub>

7172 ± 87

7172 ± 87

7172 ± 87

7172 ± 87

7172 ± 87

7172 ± 87

18 DIC<sub>pool</sub>

25158 ± 9

25182 ± 10

25628 ± 8

26295 ± 22

26637 ± 36

26953 ± 48

19 ΔTPC

-4.6 ± 15

-5.2 ± 13

-8.3 ± 13

-8.2 ± 17

-7.0 ± 13

-6.3 ± 20

20 ΔDOC

15.5 ± 58

18.3 ± 30

18.5 ± 33

25.0 ± 36

18.5 ± 73

18.1 ± 63

21 ΔDIC

5.5 ± 5.2

6.9 ± 9.2

-6.1 ± 11

-24 ± 14

-32 ± 20

-49 ± 42

22 CO<sub>2flux</sub>

4.4 ± 0.2

4.8 ± 0.3

-0.8 ± 0.5

-11 ± 1.0

-17 ± 1.4

-23 ± 2.0

23 EXP<sub>TPC</sub>

6.6 ± 0.10

5.6 ± 0.04

5.4 ± 0.07

6.0 ± 0.07

5.6 ± 0.06

6.0 ± 0.05

24 TR

107 ± 9

82 ± 7

81 ± 6

80 ± 8

75 ± 8

74 ± 8

25 BP

27 ± 8

41 ± 6

43 ± 8

41 ± 4

36 ± 5

46 ± 9

26 NPP<sub>14C</sub>

4.8 ± 0.8

11.4 ± 2.1

14.9 ± 3.6

12.3 ± 2.3

11.3 ± 2.4

14.5 ± 2.7

27 NCP<sub>o</sub>

17.4 ± 33

18.7 ± 20

15.6 ± 30

22.8 ± 28

17.1 ± 25

17.8 ± 28

28

29

Formatted: Font: 11 pt

Formatted: Font: 11 pt, Subscript

Formatted: Font: 11 pt

Formatted: Font: 11 pt, Subscript

Formatted: Font: 11 pt

Formatted: Font: 11 pt, Subscript

Formatted: Font: 11 pt

Formatted: Subscript

Formatted: Font: Italic

Formatted: Font: Italic

1 Table 2. The standing stock of total particular carbon (TPC<sub>pool</sub>), dissolved organic carbon (DOC<sub>pool</sub>) and dissolved inorganic carbon (DIC<sub>pool</sub>) at the start of  
 2 Phase II in mmol C m<sup>-2</sup> ± SE (n = 2). The net change in TPC (ΔTPC), DOC (ΔDOC) and DIC (ΔDIC) are average changes in the standing stocks during  
 3 Phase II in mmol C m<sup>-2</sup> d<sup>-1</sup> ± SE (n = 27). Flux measurements of atmospheric gas exchange (CO<sub>2flux</sub>) and exported carbon (EXP<sub>TPC</sub>) plus biological rates: total  
 4 respiration (TR), bacterial production (BP), measured (NPP<sub>14c</sub>) and net community production estimated based on organic carbon pools (NCP<sub>o</sub>), are all  
 5 average for Phase II in mmol C m<sup>-2</sup> d<sup>-1</sup> ± SE (n = [48](#), [7](#), [14](#), [5](#) and [14](#) for CO<sub>2flux</sub>, EXP<sub>TPC</sub>, TR, BP and NPP<sub>14c</sub> respectively). See Table 1 legend for further  
 6 details.

7  
 8 **Phase II (t17-t30)**

9 CO <sub>2</sub> treatment (μatm fCO <sub>2</sub> )	365	368	497	821	1007	1231
10 Mesocosm number	M1	M5	M7	M6	M3	M8
11 TPC <sub>pool</sub>	339 ± 14	337 ± 20	331 ± 22	318 ± 9	312 ± 12	339 ± 23
12 DOC <sub>pool</sub>	7435 ± 38	7483 ± 37	7487 ± 43	7597 ± 37	7487 ± 61	7479 ± 37
13 DIC <sub>pool</sub>	25247 ± 34	25269 ± 34	25639 ± 8	26177 ± 25	26413 ± 28	26757 ± 45
14 ΔTPC	-2.4 ± 5	-2.3 ± 8	-1.6 ± 14	0.3 ± 6	2.8 ± 4	3.2 ± 8
15 ΔDOC	-0.6 ± 39	2.4 ± 30	3.6 ± 40	8.4 ± 31	11.3 ± 58	9.1 ± 36
16 ΔDIC	22.4 ± 12	17.6 ± 8.1	-0.4 ± 4.5	-10.5 ± 16	-14.2 ± 10	-23.1 ± 13
17 CO <sub>2flux</sub>	1.7 ± 0.3	1.2 ± 0.3	-2.6 ± 0.3	-10 ± 0.5	-14 ± 0.6	-19 ± 1.0
18 EXP <sub>TPC</sub>	3.3 ± 0.08	2.6 ± 0.06	2.5 ± 0.08	2.6 ± 0.06	2.8 ± 0.07	2.9 ± 0.06
19 TR	140 ± 7	127 ± 5	103 ± 3	103 ± 4	101 ± 5	86 ± 4
20 BP	66 ± 17	57 ± 8	61 ± 7	57 ± 7	43 ± 6	47 ± 6
21 NPP <sub>14c</sub>	3.8 ± 0.6	11.2 ± 1.9	10.8 ± 2.0	14.3 ± 2.8	10.4 ± 2.1	12.0 ± 2.5
22 NCP <sub>o</sub>	0.3 ± 20	2.7 ± 15	4.5 ± 22	11.4 ± 16	16.9 ± 19	15.2 ± 16

23  
 24

1  
2 Table 3. The standing stock of total particular carbon (TPC<sub>pool</sub>), dissolved organic carbon (DOC<sub>pool</sub>) and dissolved inorganic carbon (DIC<sub>pool</sub>) at the start of  
3 Phase III in mmol C m<sup>-2</sup> ± SE (n = 2). The net change in TPC (ΔTPC), DOC (ΔDOC) and DIC (ΔDIC) are average changes in the standing stocks during  
4 Phase III in mmol C m<sup>-2</sup> d<sup>-1</sup> ± SE (n = ~~26~~), [using the average of the last two sampling days as the end point](#). Flux measurements of atmospheric gas exchange  
5 (CO<sub>2flux</sub>) and exported carbon (EXP<sub>TPC</sub>) plus biological rates: ~~total respiration (TR)~~, bacterial production (BP), ~~measured (NPP<sub>14C</sub>)~~ and net community  
6 production estimated based on organic carbon pools (NCP<sub>o</sub>), are all average for Phase III in mmol C m<sup>-2</sup> d<sup>-1</sup> ± SE (n = ~~137, 6, and 7~~ for [CO<sub>2flux</sub>](#), [EXP<sub>TPC</sub>](#), and  
7 [BP](#) respectively). See Table 1 legend for further details. During Phase III we did not have direct measurements of net primary production (NPP<sub>14C</sub>) or total  
8 respiration (TR).

9  
10 **Phase III (t31-t43)**

11 <b>CO<sub>2</sub> treatment (μatm fCO<sub>2</sub>)</b>	<b>365</b>	<b>368</b>	<b>497</b>	<b>821</b>	<b>1007</b>	<b>1231</b>
12 <b>Mesocosm number</b>	<b>M1</b>	<b>M5</b>	<b>M7</b>	<b>M6</b>	<b>M3</b>	<b>M8</b>
13 TPC <sub>pool</sub>	306 ± 12	304 ± 20	309 ± 20	323 ± 2	351 ± 13	384 ± 16
14 DOC <sub>pool</sub>	7426 ± 16	7469 ± 20	7485 ± 92	7553 ± 20	7593 ± 30	7562 ± 38
15 DIC <sub>pool</sub>	25557 ± 9	25545 ± 10	25648 ± 13	26030 ± 19	26197 ± 31	26371 ± 32
16 ΔTPC	-3.8 ± 10	0.3 ± 7	3.3 ± 14	3.3 ± 10	-1.4 ± 8	-4.8 ± 8
17 ΔDOC	9.8 ± 5	8.8 ± 7	8.9 ± 43	9.2 ± 10	5.7 ± 17	16.3 ± 20
18 ΔDIC	4.3 ± 3.9	5.5 ± 8.7	6.2 ± 11	-12.3 ± 7.2	-16.3 ± 14	-20.1 ± 14
19 CO <sub>2flux</sub>	-0.3 ± 0.7	-0.8 ± 0.6	-3.0 ± 0.5	-7.3 ± 0.5	-9.4 ± 0.6	-13 ± 0.6
20 EXP <sub>TPC</sub>	1.5 ± 0.07	1.4 ± 0.05	0.4 ± 0.07	1.9 ± 0.05	1.6 ± 0.04	1.7 ± 0.05
21 BP	31 ± 6.8	37 ± 1.4	38 ± 1.4	27 ± 2.1	17 ± 3.8	28 ± 2.3
22 NCP <sub>o</sub>	7.6 ± 16	10.5 ± 13	12.7 ± 20	14.3 ± 13	6.0 ± 10	13.2 ± 14

23  
24

1

## 2 **Figure legends**

3 Fig. 1. The different fractions of carbon in the control mesocosms (M1 and M5) at the start of  
4 Phase I (t0), II (t17) and III (t31) in  $\text{mmol C m}^{-2} \pm \text{SE}$  ( $n = 2$ ). The differences between the  
5 controls and elevated  $\text{CO}_2$  concentration are discussed in the text. The size of the boxes  
6 indicates the relative size of the carbon standing stocks.

7 Fig 2. The calculated exchange of  $\text{CO}_2$  between the mesocosms and the atmosphere. Positive  
8 values indicate net influx (ingassing) and negative values net outflux (outgassing) from the  
9 mesocosms. The flux was based on measurements of  $\text{N}_2\text{O}$  as a tracer gas and calculated using  
10 equations 2-5.

11 Fig 3. Change in dissolved inorganic carbon (DIC) pool and the atmospheric  $\text{CO}_2$  exchange  
12 (Fig. 2). All values are average  $\text{mmol C m}^{-2} \text{d}^{-1} \pm \text{SE}$  for the three different phases ( $n =$  [4613](#),  
13 [148](#) and [137](#) for Phases I – III respectively) in the control mesocosms (M1 + M5) and high  
14  $\text{CO}_2$  mesocosms (M3 + M8). Black, solid arrows indicated measured fluxes. Grey, dashed  
15 arrows are estimated by closing the budget, and indicate the net community production based  
16 on inorganic carbon budget ( $\text{NCP}_i$ ), which equals biological uptake or release of  $\text{CO}_2$ .

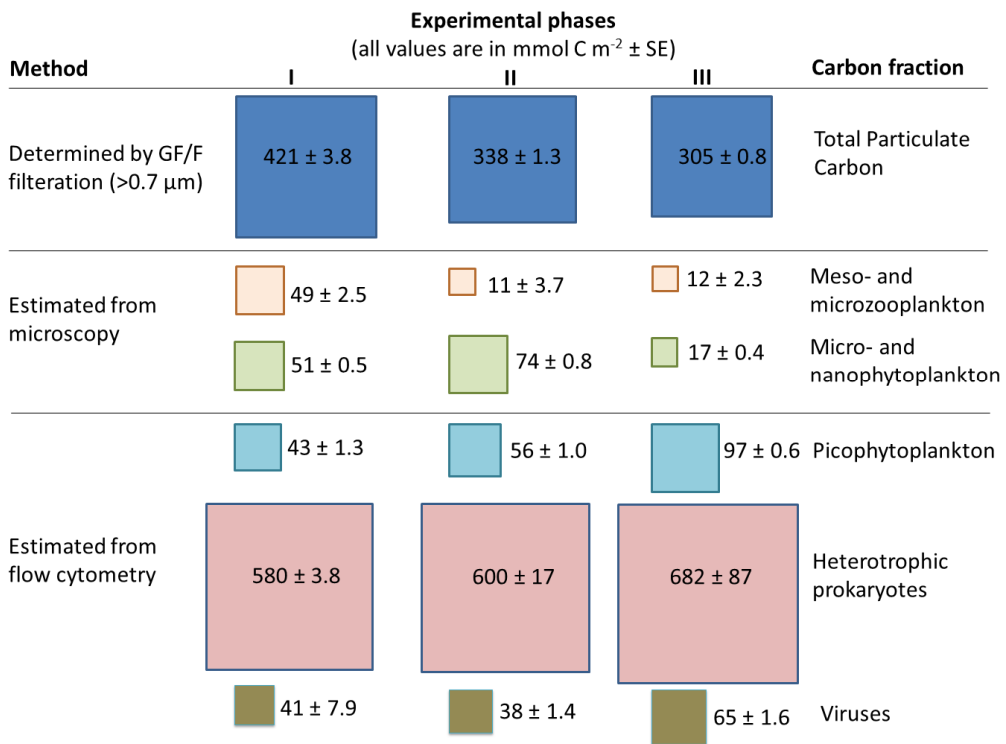
17 Fig 4. Standing stocks of total particulate carbon (TPC) and dissolved carbon (DOC) at the  
18 last day of the experiment (t43), plus the sum of exported TPC throughout the experiment; all  
19 values are in  $\text{mmol C m}^{-2} \pm \text{SE}$  ( $n = 2$ ). The values are averages of the two controls (M1 and  
20 M5) and the two highest  $\text{CO}_2$  treatments (M3 and M8). Red circles indicate statistically  
21 significant higher standing stocks in the high  $\text{CO}_2$  treatments (further details in text). The size  
22 of the boxes indicates the relative size of the carbon standing stocks and export.

23 Fig 5. Average carbon standing stocks and flow in the control mesocosms (M1 + M5) and  
24 high  $\text{CO}_2$  mesocosms (M3 + M8) during the three phases of the experiment. All carbon  
25 stocks (squares): dissolved inorganic carbon (DIC), total particulate carbon (TPC) and  
26 dissolved organic carbon (DOC), are average from the start of the period in  $\text{mmol C m}^{-2} \pm \text{SE}$   
27 ( $n = 2$ ). Fluxes (arrows) and net changes ( $\Delta$ ) are averages for the whole phase in  $\text{mmol C m}^{-2}$   
28  $\text{d}^{-1} \pm \text{SE}$  ( $n$  [presented in Table legends 1-3=2](#)). Black, solid arrows indicated measured  
29 fluxes (Tables 1-3): total respiration (TR), bacterial production (BP), exported TPC  
30 ( $\text{EXP}_{\text{TPC}}$ ). Grey, dashed arrows are estimated by closing the budget: gross primary production  
31 (GPP) using equations 7 and 8; DOC production ( $\text{DOC}_{\text{prod}}$ ) using equations 9 and 10.

1 Bacterial respiration was calculated using equation 10 and is a share of TR (indicated by the  
2 parenthesis). Aggregation was assumed to equal BP. Red circles indicate statistically higher  
3 values compared with the other CO<sub>2</sub> treatment ( $p < 0.05$ , tests presented in the primary papers  
4 described in section 2.2.). The size of the boxes indicates the relative size of the carbon  
5 standing stocks.

6

7



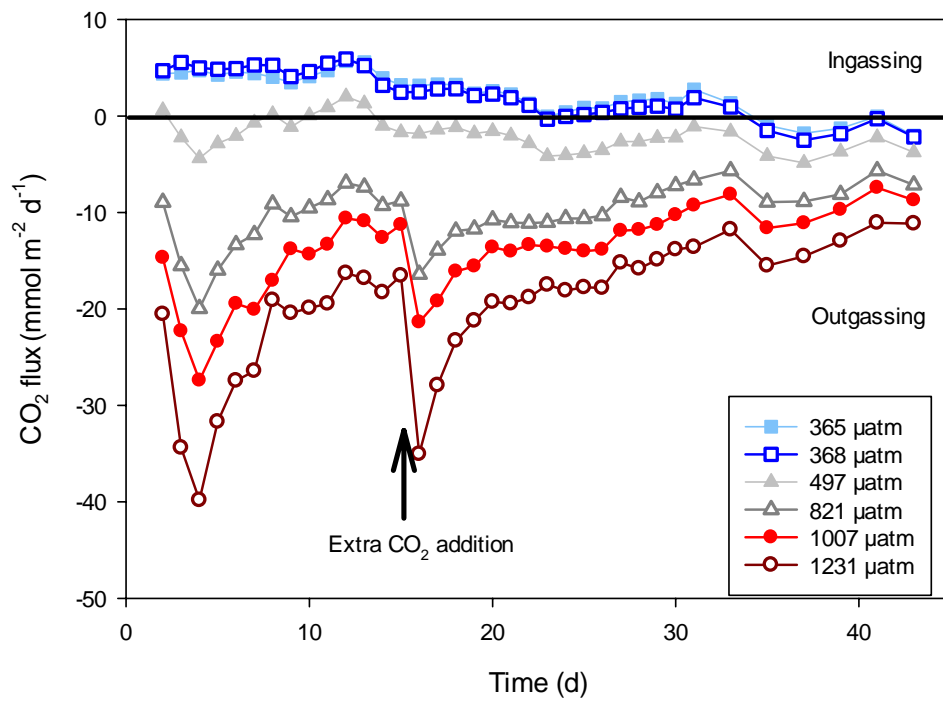
1

2 **Fig 1**

3

4





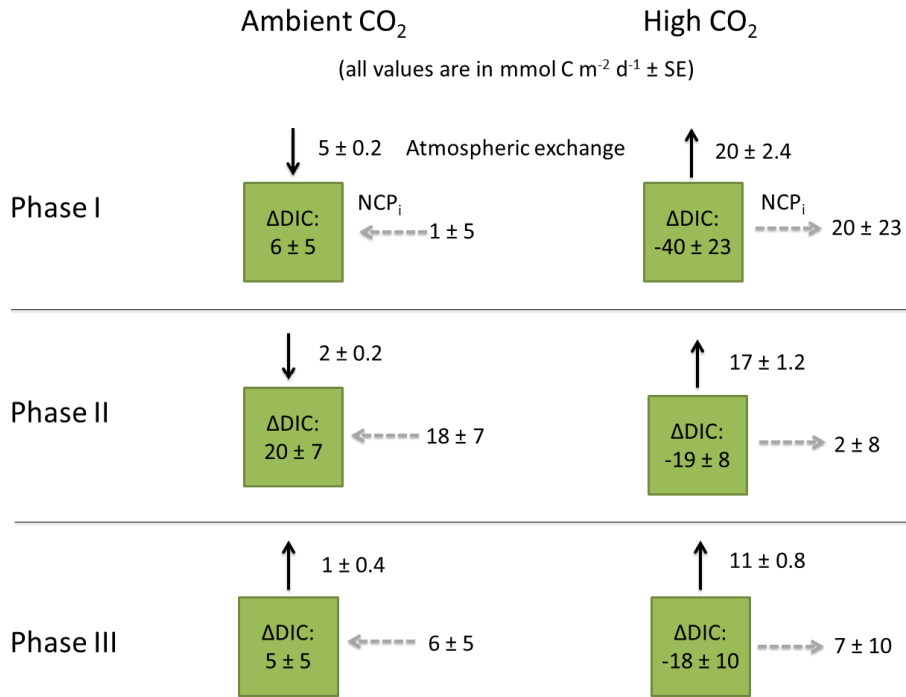
1

2 **Fig 2**

3

4

1  
2

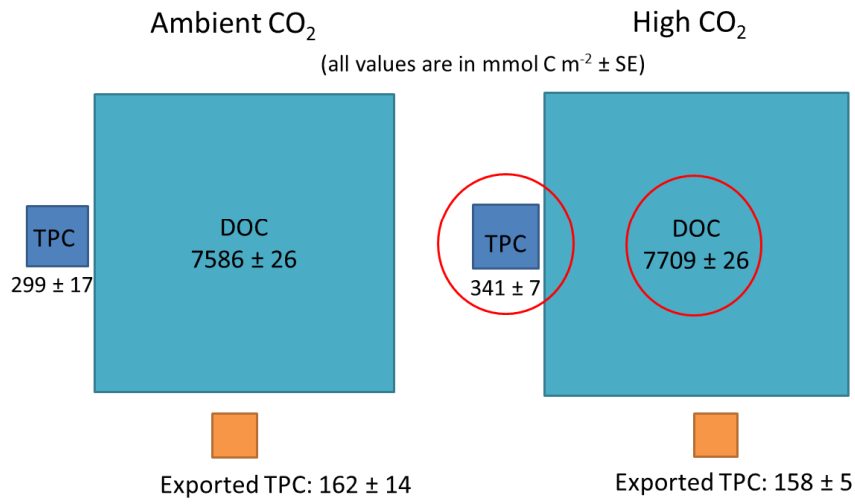


3

4 **Fig 3**

5

1



2

3 **Fig 4**

4

5

6

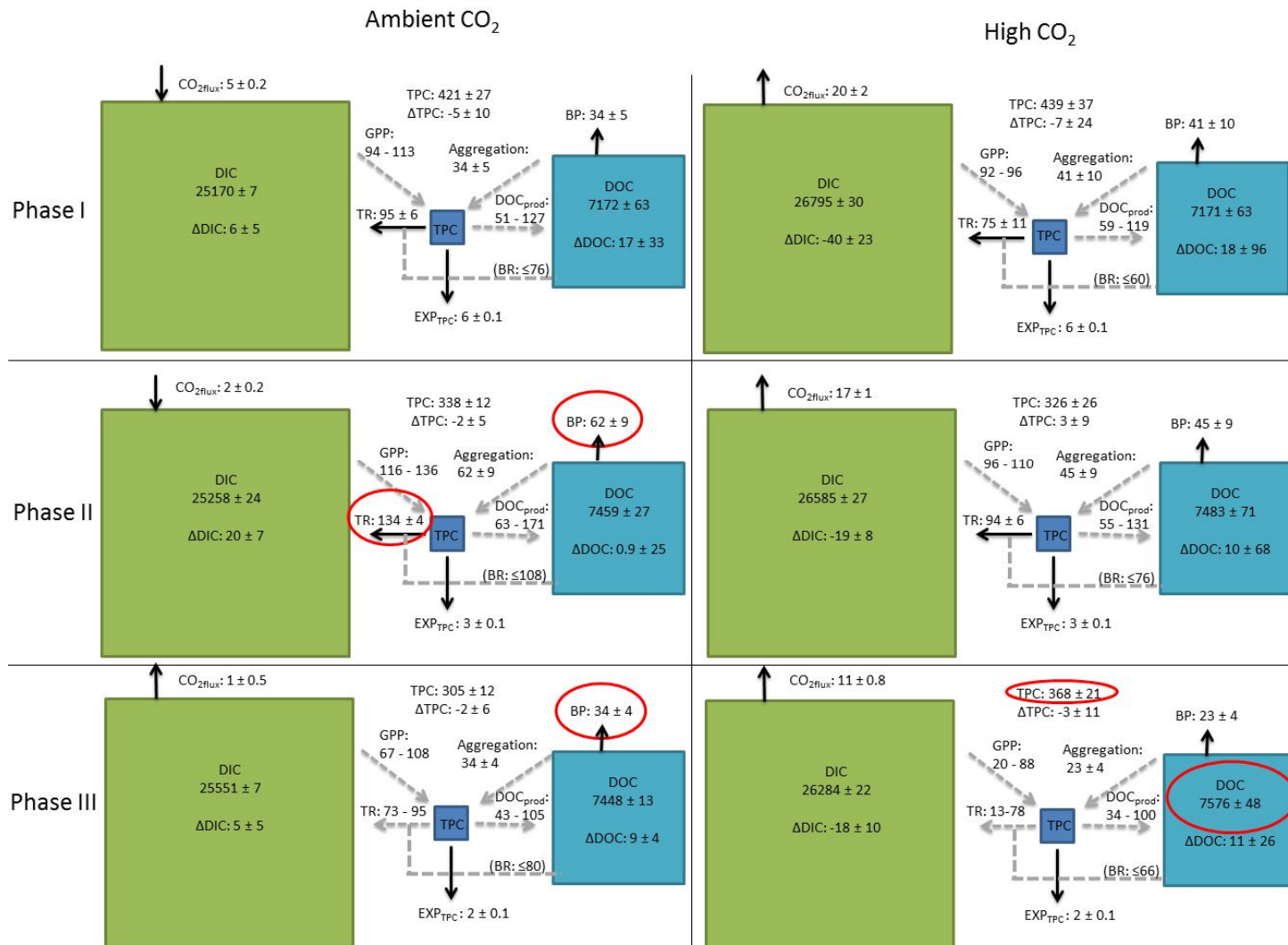


Fig 5